Available online at www.sciencedirect.com
SCIENCE DIRECT®
Ecological Modelling 191 (2006) 469–486
ECOLOGICAL MODELLING
www.elsevier.com/locate/ecolmodel

Impact of climate variability on present and Holocene vegetation: A model-based study

Jian Ni [a,b,*], Sandy P. Harrison [a,1], I. Colin Prentice [a,2], John E. Kutzbach [c], Stephen Sitch [d,3]

[a] *Max Planck Institute for Biogeochemistry, Hans Knöll Strasse 10, P.O. Box 100164, D-07701 Jena, Germany*
[b] *Laboratory of Quantitative Vegetation Ecology, Institute of Botany, Chinese Academy of Sciences, Xiangshan Nanxincun 20, 100093 Beijing, China*
[c] *Center for Climatic Research, Institute for Environmental Studies, University of Wisconsin-Madison, 1225 West Dayton Street, Madison, WI 53706-1695, USA*
[d] *Potsdam Institute for Climate Impact Research, Telegrafenberg C4, P.O. Box 601203, D-14412 Potsdam, Germany*

Received 25 October 2004; received in revised form 4 May 2005; accepted 20 May 2005
Available online 18 July 2005

Abstract

A series of nine simulations has been made with the Lund–Potsdam–Jena Dynamic Global Vegetation Model (LPJ-DGVM) in order to explore the impacts of climate variability and Holocene changes in variability (as simulated by the Fast Ocean-Atmosphere Model, FOAM) on vegetation in three forest-dominated regions of China and in the semi-arid Sahelian region of northern Africa. The simulations illustrate that changes both in the magnitude of climate variability and in the persistence of above/below average conditions have the potential to modify the vegetation response to changes in mean climate. Simulated changes in moisture availability affect vegetation through drought stress or through changing the fuel availability in semi-arid regions where lack of fuel often limits the incidence of fire. Increasing moisture availability causes trees to replace grasses in China by reducing drought stress; increasing moisture availability in the Sahel increases the available fuel and hence reduces fire return times, favouring grasses. The modelling results imply that climate variability is important to vegetation dynamics; that not only the magnitude, but also the temporal structure of variability is important; and that correctly simulating vegetation changes in response to climate variability requires a realistic "baseline" simulation of plant community composition. They further indicate

* Corresponding author. Tel.: +49 3641 576223; fax: +49 3641 577200.
E-mail address: jni@bgc-jena.mpg.de (J. Ni).
[1] Present address: School of Geographical Sciences, University of Bristol, University Road 5, Bristol BS8 1S5, UK.
[2] Present address: QUEST, Department of Earth Sciences, University of Bristol, Wills Memorial Building, Bristol BS8 1RJ, UK.
[3] Present address: Met Office (JCHMR), Maclean Building, Crowmarsh Gifford, Wallingford, Oxfordshire OX10 8BB, UK.

0304-3800/$ – see front matter
doi:10.1016/j.ecolmodel.2005.05.019

that the impacts of climate change on ecosystems can sometimes derive as much from changes in variability as from changes in mean climate.

Keywords: Climate variability; Dynamic Global Vegetation Model (DGVM); Fast Ocean-Atmosphere Model (FOAM); Fire; Foliage projective cover (FPC); Holocene; Plant functional types (PFTs)

1. Introduction

Broad-scale patterns in the distribution of natural vegetation are governed above all by climate (Holdridge, 1967; Budyko, 1974; Box, 1981; Emanuel et al., 1985; Prentice, 2001). This control is expressed in part through the tolerance limits of different plant functional types (PFTs) to climatic extremes at various stages during the growth cycle, e.g. cold tolerance, heat stress, growing-season drought (Woodward, 1987; Prentice et al., 1992). The recurrence frequency of extreme climate conditions is thus an important control on plant growth, and the long-term state of the vegetation must inevitably be determined to some degree by the interannual variability as well as by the mean climate. It also seems likely that differences in the pattern of variability – especially the tendency for extreme conditions to be repeated in consecutive years – could affect vegetation composition.

Long-term meteorological observations and reconstructions of historical climates (e.g. Karl et al., 1995; Nicholson, 2000; Higgins and Shi, 2001; Hulme, 2001; Hulme et al., 2001; Los et al., 2001) show that changes in short-term climate variability have occurred over the last few centuries. Although under current climate conditions there is a strong relationship between changes in interannual variability and changes in mean climate conditions, there is no reason why this relationship should remain fixed through time (Corti et al., 1999; Monahan et al., 2000). Further, changes in climate variability have been shown to strongly influence the regional modern vegetation distribution e.g. in Africa (Zeng et al., 1999; Plisnier et al., 2000; Wang and Eltahir, 2000; Zeng and Neelin, 2000; Oba et al., 2001) and Asia (Fu and Wen, 1999). It is therefore possible that the impacts of climate change on ecosystems could derive as much from changes in variability as from changes in the mean climate (Kutzbach et al., 2001), especially in regions with highly variable climates. On the other hand, ecosystem composition itself controls the nature of the response to a changing climate.

The palaeoclimate record shows substantial changes in mean climates during the Holocene, in response to changes in incoming solar radiation (insolation) which are predictable from known changes in the earth's orbit. These changes are most drastically illustrated by the expansion of the area influenced by the Afro-Asian summer monsoons during the early and mid-Holocene (see e.g. Street and Grove, 1976; Street-Perrott and Harrison, 1985; Street-Perrott et al., 1989; Roberts and Wright, 1993; Street-Perrott and Perrott, 1993; Winkler and Wang, 1993; Gasse and Van Campo, 1994; Jolly et al., 1998a, 1998b; Yu et al., 1998; Kohfeld and Harrison, 2000; Prentice et al., 2000a, 2000b). It is likely that these changes in mean climate were accompanied by changes in interannual to interdecadal climate variability. Accumulating palaeoclimatic evidence from the tropics suggests that El Niño-Southern Oscillation (ENSO) variability during the early to mid-Holocene was substantially less than today. Time-series of archaeological deposits in northern Peru (Sandweiss et al., 1996) and clastic deposits in an Andean lake in Ecuador (Rodbell et al., 1999) indicate less severe flooding events along the west coast of tropical South America during the early Holocene. The oxygen-isotope record from a Bolivian ice core in the tropical Andes also shows much reduced variability during the early Holocene (Thompson et al., 1998, 2000), and records of fires in Australia (McGlone et al., 1992) and isotopic records from fossil corals in the western tropical Pacific (Gagan et al., 1998) indicate that monsoon rainfall was less variable during the first half of the Holocene. But we know little about how these changes in climate variability may have affected the regional response of vegetation to climate changes in the Holocene. With the development of dynamic vegetation models (see e.g. Foley et al., 1996, 1998; Friend et al., 1997; Woodward et al., 1998; Huntingford et al., 2000; Daly et al., 2000; Bachelet et al., 2001;

Cramer et al., 2001; Kucharik et al., 2000; Sitch et al., 2003), which explicitly incorporate the effect of year-to-year variation in climate on vegetation growth and distribution, it has become possible to design model "experiments" to investigate the implications for vegetation dynamics.

In this paper we use a Dynamic Global Vegetation Model (the Lund–Potsdam–Jena, LPJ, DGVM: Sitch et al., 2003) to investigate the potential impacts of changes in interannual and interdecadal climate variability on vegetation during the Holocene. We focus on contrasting regions (China, northern Africa), both with monsoonal climates. This choice of regions was motivated by modern observations suggesting that interannual variability has a major impact on vegetation dynamics in monsoonal regions (Zeng et al., 1999; Wang and Eltahir, 2000) and palaeoenvironmental evidence for changes in variability associated with enhanced monsoon conditions in the past (Kutzbach et al., 2001). We distinguish two aspects of climate variability: the *variation* around the mean climate, and the *persistence* of above or below average conditions.

2. Methods and experimental design

We used output from control (0ka), mid-Holocene (6ka) and early Holocene (11ka) simulations made with the FOAM (Fast Ocean-Atmosphere Model: Jacob, 1997; Jacob et al., 2001) Ocean-Atmosphere General Circulation Model (OAGCM) combined with the CRU05 modern climatology (New et al., 2000) to derive synthetic climatologies with different types of variability. These synthetic climatologies were used to drive the LPJ-DGVM (Sitch et al., 2003) in order to investigate the impact of climate variability on the long-term state of the vegetation under modern, and simulated mid- and early-Holocene climates.

2.1. The FOAM model and the Holocene climate experiments

FOAM is a coupled ocean-atmosphere model designed for highly efficient use of parallel computing systems (Jacob, 1997). The atmospheric component is based on version 2 of the National Center for Atmospheric Research (NCAR) Community Climate Model (CCM2) but with the improved atmospheric physics scheme of CCM3. The atmosphere has a spectral resolution of R15 (equivalent to 4.5° latitude by 7.5° longitude). The oceanic component is developed from the Geophysical Fluid Dynamics Laboratory (GFDL) Modular Ocean Model (MOM) and has a resolution of 1.2° in latitude, 2.4° in longitude and 16 layers in the vertical. The land surface scheme uses a simple "bucket" soil hydrology model and prescribed vegetation characteristics and, therefore, does not allow for feedbacks from vegetation changes to climate; such feedbacks are now being investigated by an interactive coupling of FOAM with LPJ (Gallimore et al., 2005). FOAM was integrated for 600 years without flux corrections and showed no climate drift. Despite the relatively coarse atmospheric resolution of FOAM, the simulated present-day climate compares well with other, higher-resolution models (Jacob et al., 2001). In particular, FOAM captures most major features of the observed tropical climatology and produces realistic simulations of the modern monsoons (Jacob, 1997; Harrison et al., 2003; Liu et al., 2004). FOAM also successfully reproduces tropical climate variability, including spatial and temporal features of ENSO (Jacob, 1997; Liu et al., 1999, 2000), tropical Atlantic variability (Liu and Wu, 2000) and Pacific decadal variability (Liu et al., 2002; Wu and Liu, 2003; Wu et al., 2003).

FOAM was used to run three simulations representing the modern, mid-Holocene and early Holocene climates. The mid- and early-Holocene experiments were originally conceived as an examination of the impact of orbitally induced changes in insolation on the climate system. These simulations therefore incorporate the appropriate changes in orbital parameters (Berger, 1978) but no changes were made to atmospheric composition or to land-surface conditions (including vegetation). The atmospheric CO_2 content was set at 330 ppm, the same value as in the control simulation, in both Holocene experiments. This is considered a reasonable simplification because the present climate is not in equilibrium with the present high CO_2 concentration. The FOAM 11ka climate experiment does not include the relict Laurentide ice sheet. The impact of this ice sheet is presumed to have been geographically limited (Mitchell et al., 1988; Kutzbach et al., 1998)

and thus this simplification in the experimental design is unlikely to affect the climate or climate variability of the Afro-Asian monsoon regions, which are the focus of the current analyses.

Each of the FOAM simulations was integrated for 150 years, starting from the 450th year of an existing modern control. The last 120 years of each simulation are used to construct the model-based monthly climatologies. These climatologies were derived using the modern calendar for the control (modern) and the Holocene experiments. Although use of celestial calendar months might provide a more exact representation of climate changes during the Holocene (Kutzbach and Gallimore, 1988; Joussaume and Braconnot, 1997), in the present case the differences resulting from using the two calendars are small and unimportant (Harrison et al., 2003).

The climate values obtained from the FOAM experiments were interpolated using partial thin-plate splines (Hutchinson and Bischof, 1983; Hutchinson, 1995) from the 4.5° by 7.5° model grid to the finer grid (0.5° by 0.5°) of the CRU05 climatology and the LPJ model.

2.2. Modern climate data set

The modern climatology (mean monthly surface temperature, mean monthly precipitation and mean monthly cloud cover) was from the CRU05 (Climate Research Unit, University of East Anglia, UK) data set (New et al., 1999, 2000). This global data set provides climate statistics for every month between January 1901 and December 1998 on a 0.5° by 0.5° grid over land areas. The precipitation and temperature data were interpolated directly from meteorological station time-series to the 0.5° by 0.5° grid. Cloud cover is available from fewer individual meteorological stations. The available station data time-series were used in the interpolation wherever possible; in regions for which no cloud data is available, the gridded cloudiness values were estimated using the negative relationships between cloud cover and both diurnal temperature range and precipitation (New et al., 2000). The number of stations for each variable varies among years. For all three variables, the station data were gridded using the elevationally sensitive thin-plate smoothing spline interpolation technique (New et al., 2000).

2.3. The LPJ model

The LPJ-DGVM (Sitch et al., 2003) combines ecophysiological and ecological treatments of terrestrial vegetation dynamics, carbon and water cycling in a modular framework. The model includes the linkages and feedbacks between photosynthesis and plant water balance through canopy conductance, and the close coupling between these fast processes and representations of slower ecosystem-level processes including vegetation resource competition and production, tissue turnover, growth, establishment and mortality, soil and litter carbon turnover and the fire regime. Vegetation structure and competition are represented by nine plant functional types (PFTs) differentiated by phenology, physiology, physiognomy, disturbance-response attributes and bioclimatic constraints. Fire return intervals are represented by a fractional annual burnt area, which is predicted using an empirical function of fuel load and litter moisture (Thonicke et al., 2001).

The LPJ model is typically run, as here, at a grid resolution of 0.5° by 0.5° and driven by monthly values of temperature, precipitation and percentage sunshine hours. Atmospheric CO_2 concentration and soil texture also have to be specified. The soil texture data set is a version of the Zobler FAO soils data set originally used with the BIOME3 equilibrium vegetation model (Haxeltine and Prentice, 1996). When run with the CRU05 climatology and historical global atmospheric CO_2 concentrations, LPJ produces a good representation of the broad-scale patterns of global vegetation, and shows good agreement with observations of vegetation dynamics and the global carbon cycle over the historical period from 1901 to 1998 (Sitch et al., 2003) and during the past 20 years of Normalised Difference Vegetation Index (NDVI) and CO_2 concentration measurements (Heimann et al., 1998; Prentice et al., 2000a, 2000b; Kicklighter et al., 1999; McGuire et al., 2001; Lucht et al., 2002).

2.4. The LPJ experiments

In order to assess the impacts of changes in mean climate and in climate variability on vegetation, we made a modern LPJ control run using the CRU05 climatology and eight further experiments. The modern LPJ control simulation was initiated from a spin-up, started from

bare ground and run for 1000 model years until equilibrium was reached with respect to carbon pools and vegetation coverage. The spin-up to equilibrium required climate data with interannual variability; thus LPJ was initialised by repeating the climate sequence of the first 30 years of the CRU05 climatology. The LPJ control simulation was then continued using the CRU05 climatology from 1901 through 1998. The impact of changes in mean climate was assessed using the standard anomaly procedure (e.g. Cramer et al., 2001; Harrison and Prentice, 2003). The CO_2 concentrations for the LPJ palaeosimulations, which influence vegetation productivity, water-use efficiency and C_3–C_4 plant competition, were set to the pre-industrial CO_2 value of 280 ppm.

We considered two aspects of climate variability, the variation around the mean climate (as the standard deviation of the target variable) and the persistence of above/below average conditions (as the run length of years with a positive or negative deviation from the mean value of the target variable). The simulated variability around the mean climate at 0ka, 6ka and 11ka was derived directly from the FOAM simulations. We evaluated the role of persistence in the simulated climates by using bootstrap resampling (Efron and Tibshirani, 1993) to produce an alternative climatology with the same standard deviation but randomised with respect to timing, thus effectively removing the temporal structure of the simulated climate variability while preserving the statistical distribution of values around the mean. The temporal structure of the (real or simulated) variability may be either more regular (low persistence) or more clumped (high persistence) than random, hence the lengths of runs in the bootstrap climatology can be shorter or longer than in the corresponding simulated climate.

Thus, the derivation of the climatologies for the nine LPJ experiments was as follows:

- Experiment 1. Modern mean + modern variability (modern control run)

$$\bar{M}_i^j + (M_{i,j} - \bar{M}_i^j)$$

- Experiment 2. Modern mean + 0ka variability (0ka control run)

$$\bar{M}_i^j + (0k_{i,j} - 0\bar{k}_i^j)$$

- Experiment 3. Modern mean + bootstrap 0ka variability

$$\bar{M}_i^j + \text{bootstrapped\_resampling}(0k_{i,j} - 0\bar{k}_i^j)$$

- Experiment 4. 6ka mean + 0ka variability

$$\bar{M}_i^j + (6\bar{k} - 0\bar{k})_i^j + (0k_{i,j} - 0\bar{k}_i^j)$$

- Experiment 5. 6ka mean + 6ka variability

$$\bar{M}_i^j + (6\bar{k} - 0\bar{k})_i^j + (6k_{i,j} - 6\bar{k}_i^j)$$

- Experiment 6. 6ka mean + bootstrap variability

$$\bar{M}_i^j + (6\bar{k} - 0\bar{k})_i^j + \text{bootstrapped\_resampling}(6k_{i,j} - 6\bar{k}_i^j)$$

- Experiment 7. 11ka mean + 0ka variability

$$\bar{M}_i^j + (11\bar{k} - 0\bar{k})_i^j + (0k_{i,j} - 0\bar{k}_i^j)$$

- Experiment 8. 11ka mean + 11ka variability

$$\bar{M}_i^j + (11\bar{k} - 0\bar{k})_i^j + (11k_{i,j} - 11\bar{k}_i^j)$$

- Experiment 9. 11ka mean + bootstrap variability

$$\bar{M}_i^j + (11\bar{k} - 0\bar{k})_i^j + \text{bootstrapped\_resampling}(11k_{i,j} - 11\bar{k}_i^j)$$

where, $M_{i,j}$ is the observed CRU05 modern climatology per month ($i = 1, 2, \ldots, 12$) and per year ($j = 1, 2, \ldots, 98$); $\bar{M}_i^j$ the modern CRU05 monthly ($i = 1, 2, \ldots, 12$) mean climatology of total 98 years; $0k_{i,j}$, $6k_{i,j}$ and $11k_{i,j}$ are the FOAM simulated monthly ($i = 1, 2, \ldots, 12$) and yearly ($j = 1, 2, \ldots, 120$) climatologies at 0ka, 6ka and 11ka, respectively. $0\bar{k}_i^j$, $6\bar{k}_i^j$, $11\bar{k}_i^j$, are the FOAM simulated monthly ($i = 1, 2, \ldots, 12$) mean climatologies for total 120 years at 0ka, 6ka and 11ka, respectively; $(6\bar{k} - 0\bar{k})_i^j$ and $(11\bar{k} - 0\bar{k})_i^j$ are the differences (calculated for the each 0.5° grid cell) between the FOAM simulated 6ka and 0ka mean climatologies, and between the 11ka and 0ka mean climatologies, respectively.

2.5. Analytical framework

The analyses were focused on four regions in China and northern Africa: northeastern China (40–50°N, 115–135°E), central China (30–40°N, 95–115°E),

southern China (15–25°N, 100–125°E) and the Sahel (5–20°N, 20°W–30°E).

Foliage projective cover (FPC) was used as the index of plant abundance. To simplify the analyses, we considered five broad groups of plants: tropical evergreen woody plants, tropical raingreen woody plants, non-tropical evergreen woody plants, non-tropical summergreen woody plants, and grasses (The model does not separate forbs from grasses, and does not treat ephemeral plants). The five plant groups were aggregated from PFTs used in the LPJ model: tropical evergreen woody plants (the tropical broad-leaved evergreen woody PFT), tropical raingreen woody plants (tropical broad-leaved raingreen woody PFT), non-tropical evergreen woody plants (temperate needle-leaved evergreen woody PFT, temperate broad-leaved evergreen woody PFT and boreal needle-leaved evergreen woody PFT), non-tropical summergreen woody plants (temperate broad-leaved summergreen woody PFT and boreal summergreen woody PFT including broad-leaved and needle-leaved ones), and grasses (C_3 and C_4 herbaceous PFTs).

Extreme cold and warm temperatures and the seasonal moisture balance are considered to be the most important climate controls on the vegetation both in China (Fu and Wen, 1999; Ni et al., 2000) and in northern Africa (Zeng and Neelin, 2000). We use the mean temperature of the coldest month (MTCO) as an index for extreme cold temperatures, the mean temperature of the warmest month (MTWA) as an index for extreme warm temperatures, and two precipitation measures to assess the seasonal moisture balance: mean annual precipitation (MAP) and mean summer precipitation (MSP, where summer is defined as May through September).

3. Results

3.1. Characteristics of the observed and simulated climates

There are noticeable model biases, i.e. differences between the simulated and observed modern climates (Table 1). Winter temperatures are lower in the FOAM control run than observed (Table 1) in all regions of China. Simulated summer temperatures are also lower than observed, particularly in northeastern and central China. Summer and mean annual precipitation are overestimated compared to observed values in northeastern and central China: the discrepancy is most noticeable in central China where simulated rainfall values are about 3.5 times larger than observed. In contrast, simulated rainfall is slightly less than observed in southern China. Winter and summer temperatures are also significantly lower in the FOAM control run than observed (Table 1) in the Sahel. Simulated precipitation is less than observed in the Sahel. Joussaume et al. (1999) indicated, from an evaluation of climate simulations of 6ka made with seventeen climate models, that the magnitude of the insolation-induced changes in climate is partially determined by the magnitude of the biases in the control simulation. Our derived palaeoclimatologies therefore probably do not realistically capture the climate response to orbital forcing in the early- to mid-Holocene and we may underestimate the vegetation response, but this problem does not affect our qualitative conditions.

Characteristics of simulated variability also differ somewhat from observed variability patterns (Fig. 1). In general, FOAM tends to underestimate interannual variability in both summer and winter temperature (Table 1). There is no systematic pattern to the relationship between observed and simulated precipitation variability: in southern China and the Sahel, the simulated variability is similar to the observed variability, in northeastern China the simulated variability is underestimated, and in central China it is overestimated.

3.2. Vegetation response to changes in mean climate and climate variability

3.2.1. Northeastern China

The early to mid-Holocene insolation regime increased the seasonal contrast in temperature, leading to simulated warmer summers and generally colder winters across most of China (Table 1). These changes in the mean climate state (experiments 4 and 7) produced a simulated reduction in both evergreen and summergreen forests in northeastern China between experiments 2 and 4, and between experiments 2 and 7, principally as a result of increased summer heat reducing the viability of the boreal PFTs which are dominant in this region. Reduced tree competition allowed grasses to expand (Fig. 2a). However, the simulated summer warming was accompanied by a reduction in

Table 1
Simulated changes in mean climate and climate variability during the Holocene

Region	Time	Mean annual precipitation (MAP, mm)				Mean summer (May–September) precipitation (MSP, mm)				Mean temperature of the coldest month (MTCO, °C)				Mean temperature of the warmest month (MTWA, °C)			
		Regional mean	Regional S.D.	Run length	Bootstrap run length	Regional mean	Regional S.D.	Run length	Bootstrap run length	Regional mean	Regional S.D.	Run length	Bootstrap run length	Regional mean	Regional S.D.	Run length	Bootstrap run length
Northeastern China	Modern	532.8	195.4	1.88		402.1	138.3	2.04		−20.2	4.87	2.33		20.9	2.07	2.45	
	0ka	**603.9**	**116.3**	2.35	2.03	**449.3**	**82.0**	2.03	2.03	**−38.1**	**4.19**	1.93	2.14	**10.4**	**1.82**	1.97	1.67
	6ka	*653.9*	*105.0*	2.18	1.71	*510.9*	81.8	1.97	1.76	*−37.6*	*3.74*	1.85	1.69	*13.2*	*1.74*+	1.93	1.85
	11ka	*674.9**	114.3*	1.64	2.00	*536.3**	*93.0**	1.79	2.14	*−39.0**	*3.81*	1.90	2.07	*15.5**	*1.69*	2.31	1.90
Central China	Modern	482.8	284.9	1.92		335.3	188.1	1.78		−7.5	6.63	2.39		18.9	7.40	3.38	
	0ka	**1568.5**	**596.7**	2.03	2.40	**1170.6**	**422.7**	2.10	2.22	**−21.8**	**3.81**	2.03	2.37	**11.8**	**3.38**	2.03	1.46
	6ka	*1584.2*+	*586.5*+	2.10	2.26	*1221.0*	*447.4*	2.26	2.07	*−22.4*	3.86	2.14	1.90	*13.7*	3.35	2.22	2.07
	11ka	*1638.7**	*579.1*	1.85	2.03	*1294.8**	*462.4**	1.74	2.10	*−23.4**	3.82	2.03	1.76	*15.4**	*3.22**	1.76	1.93
Southern China	Modern	1680.3	517.0	1.85		1077.7	317.4	1.92		15.1	4.73	2.58		26.9	2.53	2.72	
	0ka	**1441.0**	**500.2**+	2.07	2.00	**935.8**	317.9	1.87	2.00	**5.7**	**6.96**	1.97	2.40	**24.2**	**3.17**	1.87	1.76
	6ka	*1410.6*	*474.3*	1.90	2.03	*972.9*	*328.6*+	2.00	2.00	*3.5*	7.04	1.87	2.03	*24.9*	*2.93*	2.55	2.03
	11ka	1438.5*	486.9	1.90	1.74	*1003.2**	*330.8*	1.76	1.79	*2.7**	7.00	2.10	2.07	*26.2**	*2.83**	1.90	1.90
Sahel	Modern	711.8	634.3	4.67		489.7	400.6	2.51		22.1	2.86	2.18		31.6	1.04	2.80	
	0ka	**594.7**	644.8	1.76	2.14	**472.4**	**495.4**	2.03	1.85	**14.8**	**4.85**	2.67	1.82	**28.4**	**0.33**	2.03	1.85
	6ka	*688.7*	*631.7*	2.22	1.94	*579.8*	*513.6*	2.31	1.71	*13.6*	*5.11*	2.79	1.94	*28.1*	*1.57*	2.14	1.90
	11ka	*710.9**	*632.1*	1.94	2.00	*610.9**	*524.0**	1.97	1.97	*12.6**	*5.13*	2.31	2.55	*29.0**	*1.75**	2.03	2.07

The four regions: northeastern China (40–50°N, 115–135°E), central China (30–40°N, 95–115°E), southern China (15–25°N, 100–125°E) and the Sahel (5–20°N, 20°W–30°E). The regional mean value is the spatial average of the 98-year or 120-year mean of the climate variable for each grid cell in a region. The regional standard deviation (S.D.) is the mean S.D. of the regional means. Run length (and bootstrap run length) is defined as the number of years of climate data (98 years for modern climatology and 120 years for climatic simulations) divided by the number of transitions between positive and negative deviations from the mean. Numbers in bold indicate that the simulated 0ka values are significantly different from modern observations; numbers in italics indicate that 6ka and/or 11ka are significantly different from the 0ka control values; numbers marked by *indicate that simulated 11ka and 6ka values are significantly different from one another (all at 95% confidence interval, using the paired-samples *t*-test in SPSS 11.0). Numbers marked by +indicates that differences are significant only with 90% confidence.

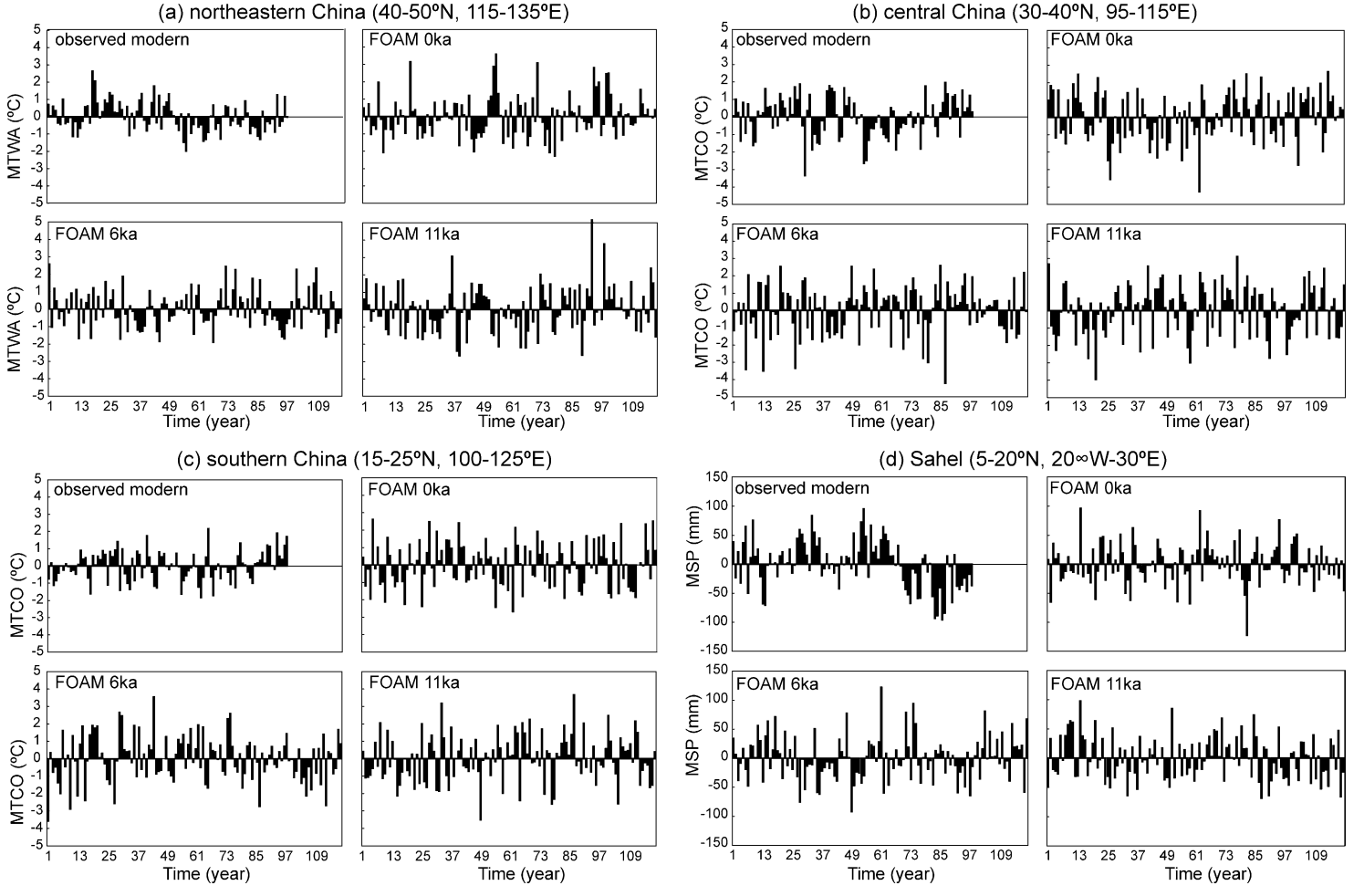

Fig. 1. Year-to-year deviations of the annual regional means of the major driving climate variables from the multiannual mean for four regions. The major driving variables are taken to be the mean temperature of the warmest month (MTWA) in northeastern China, the mean temperature of the coldest month (MTCO) in central and southern China, and the mean summer precipitation from May to September (MSP) in the Sahel. The time span is 98 years for the modern observations and 120 years for the FOAM simulations of 0ka, 6ka and 11ka.

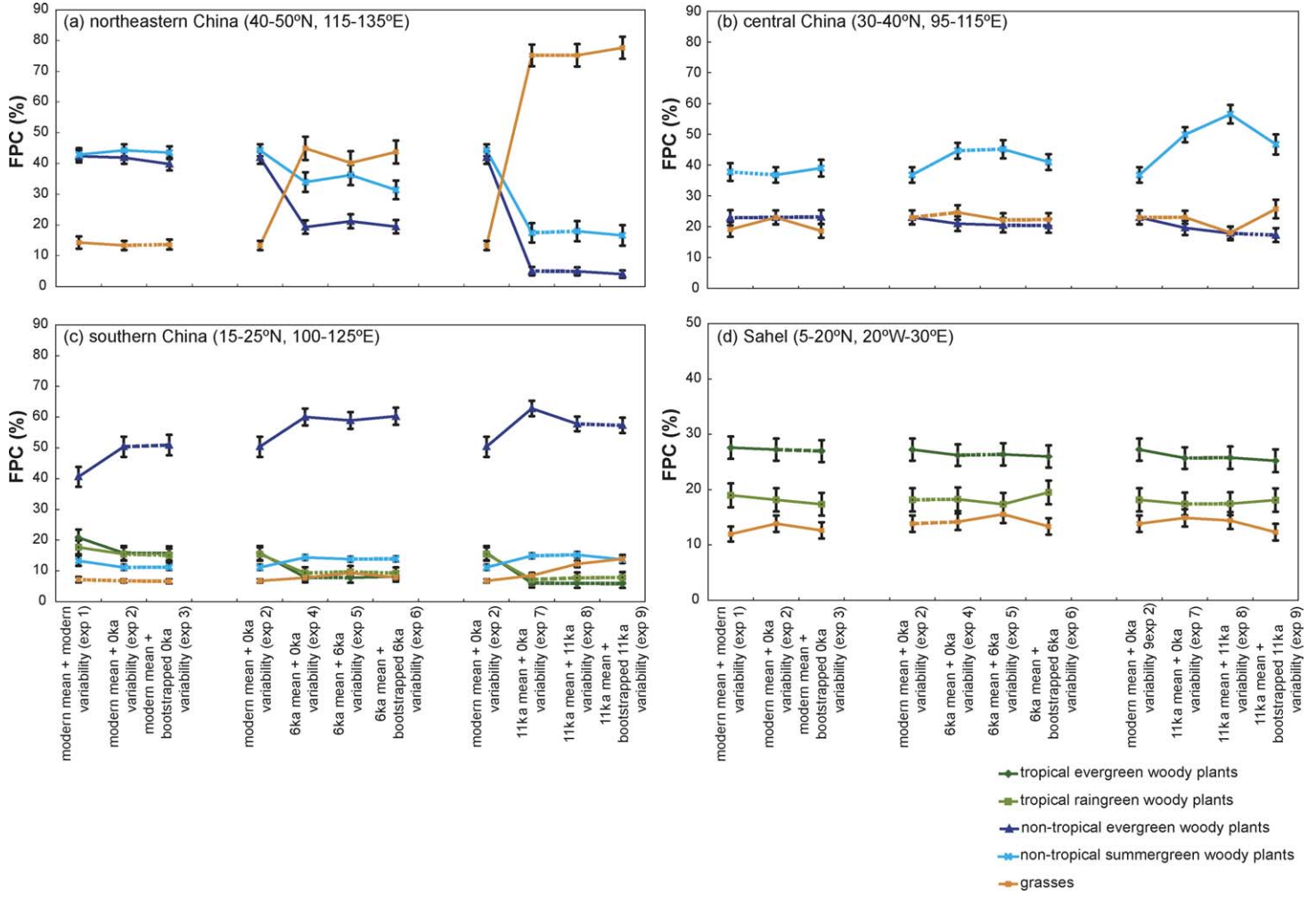

Fig. 2. Response of vegetation (foliage projective cover, FPC) to changes of mean climates and climate variability for four regions. The FPC values are averaged from the 98-year or 120-year means of annual FPC values for each grid cell across a region. Standard deviation (S.D.) of FPC in each region was divided by 10. Solid line: significant different between two experiments at 95% confidence; long dashed line: significant different between two experiments at 90% confidence; short dashed line: no significant different between two experiments. Note that changes in the Sahel (d) are smaller than in the other regions and the scale of this plot is therefore different from the scale of (a), (b), (c).

interannual variability. At 6ka, this reduced variability (experiment 5) was sufficient to counteract, to some degree, the tendency for forest expansion between experiments 4 and 5 (Fig. 2a) by reducing the occurrence of extreme warm years. At 11ka, however, the simulated reduction in variability (experiment 8) was insufficient to offset the impact of the considerably larger increase in MTWA and there was no significant change in the relative abundance of grasses and trees between experiments 7 and 8.

The temporal structure of the variability was shown also to be important in determining the vegetation response. When the persistence of runs of warmer/colder summers was reduced by bootstrapping, grasses increased at the expense of trees between experiments 5 and 6, and between experiments 8 and 9 (Fig. 2a). This behaviour reflects the fact that the length of time during which boreal trees are subject to extreme summer conditions is important: for example, trees that are stressed for several years in succession are more likely to die than those that are stressed during a single summer. The effect is present in the 0ka simulation but muted because heat stress is infrequent; the simulations indicate a stronger effect for the Holocene.

3.2.2. Central China

Simulated summer temperatures in central China were higher during the mid- and early-Holocene. The simulated summer warming was accompanied by winter cooling (Table 1). The increased seasonality and colder winters (experiments 4 and 7) produced a simulated increase in summergreen trees at the expense of the (predominantly) temperate broad-leaved evergreen trees between experiments 2 and 4, and between experiments 2 and 7 (Fig. 2b). There was no significant change in interannual temperature variability between the 6ka (experiment 5) and 0ka control simulations. However, the variability in summer temperatures (MTWA: Table 1) was reduced in the 11ka simulation (experiment 8) compared to the 0ka control and, as a result, summergreen trees increased and grasses became less abundant between experiments 7 and 8 (Fig. 2b).

Changes in the temporal structure of the variability influenced the vegetation through the competitive balance between summergreen trees and grasses. Increased lengths of runs of above/below average cold years (MTCO) under modern mean climate conditions favour summergreen trees between experiments 2 and 3, while decreased lengths of above/below average cold years (MTCO) in the Holocene simulations produced a reduction in the abundance of summergreen trees and an increase in the abundance of grasses between experiments 5 and 6, and between experiments 8 and 9 (Fig. 2b).

3.2.3. Southern China

Increased seasonality and colder winters in southern China in the Holocene simulations (Table 1) led to an increase in temperate trees (both evergreen and summergreen) at the expense of tropical trees between experiments 2 and 4, and between experiments 2 and 7 (Fig. 2c). There was no significant change in the variability of MTCO between the Holocene and control simulations. Nevertheless, a slightly increased abundance of grasses and reduced abundance of tropical raingreen trees between experiments 4 and 5 and between experiments 7 and 8 occurred in the simulations that took changed variability into account. This change may be related to the simulated increased variability in summer rainfall (Table 1), which favours (short-lived) grasses over longer-lived trees. Removing the temporal structure of the variability (experiments 5 and 6, and experiments 8 and 9) had little impact in this region (Fig. 2c).

3.2.4. The Sahel

Insolation-induced changes in the African monsoon resulted in increased summer and total annual precipitation in the Sahel, in both the Holocene simulations (Table 1). These changes in the mean climate (experiments 4 and 7) resulted in increased abundance of grasses (Fig. 2d). Tropical evergreen shrubs decreased in abundance in the 6ka simulation, and both evergreen and raingreen shrubs decreased in abundance in the 11ka simulation between experiments 2 and 4, and between experiments 2 and 7 (Fig. 2d). The decline in shrubby vegetation is a fire-related response. Fire return intervals are relatively long under modern conditions in much of the Sahel because the sparsity of vegetation limits fuel availability, restricting the spread of fires. As the simulated climate becomes wetter, vegetation cover increases and hence fuel load increases and fires become more frequent (Table 2). More frequent fires in turn favour short-lived grasses over the longer-lived shrubs. The increase in simulated Holocene mean

Table 2
Simulated fire return interval (FRI, years) and total foliage projective cover (FPC, %) in the four regions and nine modelling experiments

		Modern mean			6ka mean			11ka mean		
		Modern variability	0ka variability	Bootstrap 0ka variability	0ka variability	6ka variability	Bootstrap 6ka variability	0ka variability	11ka variability	Bootstrap 11ka variability
Northeastern China	FRI	148.0	162.0	162.1	238.2	232.8	235.2	448.7	429.1	439.7
	FPC	99.6	99.6	97.0	98.3	97.7	94.6	97.6	98.1	98.3
Central China	FRI	75.4	79.7	79.7	112.7	114.4	113.0	127.9	134.1	136.1
	FPC	79.9	82.9	80.9	90.4	87.9	83.7	92.6	92.4	89.8
Southern China	FRI	91.6	83.4	82.8	83.5	79.0	83.1	86.8	85.0	86.5
	FPC	99.5	99.6	99.5	99.5	99.5	99.6	99.5	99.0	98.7
Sahel	FRI	72.1	91.0	90.6	83.9	75.8	74.4	83.2	75.1	75.4
	FPC	58.9	59.6	57.3	59.3	60.0	59.5	59.2	58.5	56.6

precipitation in the Sahel was accompanied by an increase in interannual variability (Table 1). At 6ka, this increase favours grasses at the expense of raingreen shrubs between experiments 4 and 5 (Fig. 2d). At 11ka, the increased variability produces no effect on the shrub population but a decrease in the abundance of grasses between experiments 7 and 8. A reduction in the persistence of above/below average rainfall by randomisation favours raingreen shrubs over evergreen shrubs or grasses in both the Holocene simulations between experiments 5 and 6, and between experiments 8 and 9 (Fig. 2d).

4. Discussion

These model experiments suggest that, in general, changes in the mean climate state between Holocene simulations and the modern control simulation had a larger impact on regional vegetation than changes in the amount or pattern of climate variability. Nevertheless, simulated changes in both the magnitude of interannual variability and in the persistence of above/below average conditions had a statistically significant impact on vegetation in most regions (Fig. 2), and in certain cases the effect on vegetation resulting from a change in variability was as large as the effect of a change in the mean climate. In central China, for example, the change in the FPC of temperate summergreen trees caused by modifying the temporal structure of 11ka variability (Fig. 2b) was of similar magnitude to the change caused by the 11ka mean climate.

These results do not necessarily indicate the relative importance of changes in mean climate and climate variability in explaining *observed* vegetation changes between the early to mid-Holocene and the present. This is because there are fairly large regional biases in both the mean climate and the variability of the 0ka control simulation; such biases probably affect the magnitude of the response to changes in climate forcing (Joussaume et al., 1999). Furthermore, the FOAM simulations do not incorporate feedbacks associated with e.g. vegetation changes and changes in atmospheric aerosol loadings that are known to have a significant impact on the simulation of tropical and subtropical climates (Broström et al., 1998; Braconnot et al., 1999; Kutzbach et al., 2001; Claquin et al., 2003). Indeed, several aspects of the simulations are

inconsistent with pollen-based palaeovegetation reconstructions. The simulated increase in non-tropical summergreen woody plants in central China (Fig. 2b) and the simulated increase in non-tropical evergreen woody plants in southern China (Fig. 2c) at 6ka occurs at the expense of temperate broad-leaved woody plants and tropical woody plants respectively. This implies a southward shift in the vegetation belts which is inconsistent with the observed northward expansion of both temperate deciduous broad-leaved forest and warm-temperate forests at 6ka shown by pollen data (Yu et al., 1998, 2000; Ni et al., 2005). These inconsistencies arise because FOAM simulates winter cooling over most of China; the observations imply that the winters were warmer at 6ka. The expansion of grasses in northeastern China (Fig. 2a) is also not consistent with the pollen-based reconstructions, which show a slight expansion of forests into the continental interior. Analysis of the response of coupled ocean-atmosphere models to 6ka insolation forcing shows that these models produce more arid conditions in mid-continental Eurasia and an unrealistic expansion of grasslands (Wohlfahrt et al., 2004, 2005). The FOAM 6ka simulation shows a similar response to insolation forcing. The simulated decrease in both raingreen and evergreen woody plants in the Sahel is also not consistent with pollen-based reconstructions which show northward extension of both xerophytic shrubland and grassland in the Sahel/Sahara during the early Holocene (Jolly et al., 1998a) and mid-Holocene (Jolly et al., 1998a, 1998b). Climate model simulations of the response to 6ka orbital forcing consistently underestimate the expansion of the African monsoons (Joussaume et al., 1999) and, although ocean feedbacks amplify the monsoon changes (Hewitt and Mitchell, 1998; Braconnot et al., 2000; Kutzbach et al., 2001), analysis of coupled ocean-atmosphere simulations show that none of the current models produces a sufficiently large increase in mean precipitation or a sufficiently large northward displacement of the monsoon front at 6ka (Braconnot et al., 2004). It is likely that more realistic simulation of continental climates of the Holocene, including the paradoxical winter warming shown by the observations from several regions of Eurasia, will have to take vegetation feedbacks into account (e.g. Bonan et al., 1992; Ganopolski et al., 1998; Berger, 2001; Claussen, 2001; Wohlfahrt et al., 2004). Even if the simulations produced changes that are consistent with observed vegetation changes, independent evidence for changes in high-frequency climate variability would be required to determine whether both the mean climate changes and the changes in variability were correct. Palaeoenvironmental data from tropical South America and Australasia do show reduced high-frequency variability in the ENSO domain during the early to mid-Holocene (e.g. McGlone et al., 1992; Shulmeister and Lees, 1995; Gagan et al., 1998; Tudhope et al., 2001) but there is no direct evidence for high-frequency variability changes in the Sahel or China. Under modern conditions, Sahelian precipitation is correlated with ENSO and thus the observed reduction in ENSO during the early to mid-Holocene could be construed as inconsistent with the simulated increase in precipitation variability shown in the FOAM simulations. However, climate-model simulations show that ENSO teleconnection patterns may have been different during the early- to mid-Holocene (Otto-Bliesner, 1999) and thus changes in the core ENSO region may not be a good guide to changes in the Sahel or in China (Bradley et al., 2003). Given these constraints, our aim in this paper is not to examine the relative importance of mean climate change and climate variability during a specific interval in the past, but rather to establish whether climate variability could have important impacts of vegetation and to explore the mechanisms whereby these impacts are expressed.

Our analyses show that changes in interannual variability in both summer and winter temperatures can produce significant changes in vegetation. Several physiological mechanisms enable plants to survive temperature extremes (Raunkiaer, 1934; Gauslaa, 1984; Woodward, 1987, 1988; Woodward and Kelly, 1997; Gurvich et al., 2002; Larcher, 2003). Increases in high-frequency climate variability increase the chances of a given lethal temperature threshold being exceeded, and thus lead to decrease in the abundance of that PFT. This effect can be seen e.g. in the simulations for central China at 11ka, where the increased interannual variability in MTCO produces a decrease in evergreen woody plants and thereby allows summergreen woody plants to increase in abundance. However, changes in the temporal structure of temperature variability also have an impact on the abundance of specific woody PFTs (see e.g. northeastern China, central China). For changes in the persistence of above/below average temperatures to have an impact on woody PFT abundance, there must be some implicit preconditioning which means

that plants that experience suboptimal conditions for several years are more likely to die than those that experience extreme conditions only occasionally.

Our analyses show that changes in the interannual variability of precipitation are important in determining changes in the simulated vegetation in northeastern China and in the Sahel. The response of vegetation to changes in the interannual variability of precipitation is complex, because changes in precipitation cause changes in both the incidence of drought stress and in the fire regime. Increasing moisture availability, by reducing the incidence of drought stress, tends to favour the replacement of grass by woody vegetation. However, increasing moisture availability also tends to increase fuel load. Under conditions when fuel is the limiting constraint on fire frequency, as it is in the Sahel region in our simulations, increasing moisture availability increases the incidence of fires; the short fire-return time in turn favours grass over woody vegetation. Thus, changes in moisture availability and its variability are expected to have quite different effects in different regions, depending on the type of vegetation present and factors governing fire disturbance.

Modern studies of fire ecology in a variety of different vegetation types have shown that the incidence of fires is strongly controlled by climate conditions in the previous season which determines the existence of a sufficient fuel load (Goldammer and Seibert, 1990; Justice et al., 1996; Olson et al., 1999; Grau and Veblen, 2000). However, in more humid environments where fuel load is not limited, fire-ecology studies show no correlation between preceding climate conditions and the incidence of fire; rather fire incidence is directly correlated with the existence of drought during the growing season (Hessl et al., 2004). These observations are consistent with our inference that increased moisture availability will promote fires in fuel-limited regions but suppress fires in regions where there is already sufficient fuel.

The impact of changes in the persistence of drought also appears to be dependent on the baseline state of the climate and the type of vegetation present. Decreasing the length of droughts in simulations for the Sahel allowed raingreen shrubs to increase in abundance at the expense of grasses. A similar decrease in the length of droughts in northeastern China, however, led to increased grass cover because the expansion of woody vegetation there is limited by low winter temperatures.

Different types of model have been used to study the response of vegetation to climate change, from equilibrium vegetation models (e.g. Prentice et al., 1992; Neilson, 1995; Haxeltine and Prentice, 1996) through dynamic vegetation models (e.g. Claussen, 1996; Foley et al., 1998; Cramer et al., 2001; Sitch et al., 2003) and earth system models which couple the dynamic response of vegetation to ocean-atmosphere general circulation models (Cox et al., 2000; Huntingford et al., 2000; Doherty et al., 2000; Gallimore et al., 2005). Equilibrium vegetation models normally implicitly assume that the relationship between changes in mean climate state and climate variability is related, whereas dynamic vegetation models can explicitly take climate variability (and its impact on disturbance regimes) into account. Our analyses suggest that climate variability can be an important determinant of the mean state of the vegetation at a regional scale. One implication of these findings is that, in so far as the relationship between changes in mean climate and in climate variability is not fixed, studies of the response of vegetation to climate change require the use of dynamic vegetation models. Given that the response to variability is conditioned by the mean climate, the magnitude of the variability and the persistence characteristics of the variability, our findings also pose a challenge for climate modelling. In order to predict the response of vegetation to climate changes, it will be necessary to predict both the magnitude and the structure of short-term climate variability correctly. This will have a further impact because modelling studies have indicated that vegetation dynamics may reciprocally affect climate variability. Studies of vegetation feedbacks in the Sahel, for example, have shown that changes in vegetation cover caused by rainfall variability are themselves involved in generating interdecadal persistence of wet or dry states (Zeng et al., 1999; Wang and Eltahir, 2000). In this paper, we have considered only the response of vegetation dynamics to climate variability using a one-way coupling of models. Future work will also need to consider the feedbacks between vegetation and climate on interannual to interdecadal time scales (Prentice, 2001).

Acknowledgements

The FOAM simulations were supported by the National Science Foundation (NSF), Climate

Dynamics and Earth System History Programs, and by computer resources provided by the National Center for Atmospheric Research (NCAR), Boulder, Colorado, and by the National Center for Supercomputer Applications (NCSA), University of Illinois. The CRU05 monthly climate data were supplied by the Climate Impacts LINK Project (UK Department of the Environment Contract EPG 1/1/16) on behalf of the Climate Research Unit, University of East Anglia, UK. We would like to thank Kerstin Sickel for technical assistance, and Natalia Ungelenk and Silvana Schott for editorial assistance. JN would also like to thank the National Natural Science Foundation of China (NSFC 90102009), the Chinese Academy of Sciences (KZCX1-10-05), the Max Planck Society (MPG) and the Max Planck Institute for Biogeochemistry (MPI-BGC) in Germany, for research and visit funding. This work was begun while JEK was a Humboldt Visiting Fellow at the MPI-BGC. This work is a contribution to the TEMPO (Testing Earth-system Models with Palaeoenvironmental Observations) project.

References

Bachelet, D., Lenihan, J.M., Daly, C., Neilson, R.P., Ojima, D.S., Parton, W.J., 2001. MC1: a dynamic vegetation model for estimating the distribution of vegetation and associated ecosystem fluxes of carbon, nutrients and water. General Technical Report PNW-GTR-508. US Department of Agriculture, Forest Service, Pacific Northwest Research Station, Portland, OR, 101 pp.

Berger, A., 1978. Long term variations of daily insolation and quaternary climate changes. J. Atmos. Sci. 35, 2362–2376.

Berger, A., 2001. The role of CO_2, sea level and vegetation during the Milankovitch-forced glacial-interglacial cycles. In: Bengtsson, L.O., Hammer, C.U. (Eds.), Geosphere–Biosphere Interactions and Climate. Pontifical Academy of Sciences, Cambridge University Press, Cambridge, pp. 119–146.

Bonan, G.B., Pollard, D., Thompson, S.L., 1992. Effects of boreal forest vegetation on global climate. Nature 359, 716–718.

Box, E.O., 1981. Macroclimate and Plant Forms: An Introduction to Predictive Modeling in Phytogeography. W. Junk Publishers, The Hague, 258 pp.

Braconnot, P., Harrison, S.P., Joussaume, S., Hewitt, C.D., Kitoh, A., Kutzbach, J., Liu, Z., Otto-Bliesner, B.L., Syktus, B., Weber, S.L., 2004. Evaluation of coupled ocean-atmosphere simulation of the mid-Holocene. In: Battarbee, R.W., Gasse, F., Stickley, C.E. (Eds.), Past Climate Variability through Europe and Africa. Kluwer Academic Publishers, Dordrecht, pp. 513–553.

Braconnot, P., Joussaume, S., de Noblet, N., Ramstein, G., 2000. Mid-Holocene and Last Glacial Maximum African monsoon changes as simulated within the Paleoclimate Modelling Intercomparison Project. Glob. Planet. Change 26, 51–66.

Braconnot, P., Joussaume, S., Marti, O., de Noblet, N., 1999. Synergistic feedbacks from ocean and vegetation on the African monsoon response to mid-Holocene insolation. Geophys. Res. Lett. 26, 2481–2484.

Bradley, R.S., Briffa, K.R., Cole, J., Hughes, M.K., Osborn, T.J., 2003. The climate of the last millennium. In: Alverson, K.D., Bradley, R.S., Pedersen, T.F. (Eds.), Paleoclimate, Global Change and the Future. Springer-Verlag, Berlin, Heidelberg, pp. 105–141.

Broström, A., Coe, M., Harrison, S.P., Gallimore, R., Kutzbach, J.E., Foley, J., Prentice, I.C., Behling, P., 1998. Land surface feedbacks and palaeomonsoons in northern Africa. Geophys. Res. Lett. 25, 3615–3618.

Budyko, M.I., 1974. Climate and Life. Academic Press, New York, 608 pp.

Claquin, T., Roelandt, C., Kohfeld, K.E., Harrison, S.P., Prentice, I.C., Balkanski, Y., Bergametti, G., Hansson, M., Mahowald, N., Rodhe, H., Schulz, M., 2003. Radiative forcing effect of ice-age dust. Clim. Dyn. 20, 193–202.

Claussen, M., 1996. Variability of global biome patterns as a function of initial and boundary conditions in a climate model. Clim. Dyn. 12, 371–379.

Claussen, M., 2001. Biogeophysical feedbacks and the dynamics of climate. In: Schulze, E.-D., Heimann, M., Harrison, S.P., Holland, E., Lloyd, J., Prentice, I.C., Schimel, D.S. (Eds.), Global Biogeochemical Cycles in the Climate System. Academic Press, San Diego, pp. 61–69.

Corti, S., Molteni, F., Palmer, T.N., 1999. Signature of recent climate change in frequencies of natural atmospheric circulation regimes. Nature 398, 799–802.

Cox, P.M., Betts, R.A., Jones, C.D., Spall, S.A., Totterdell, I.J., 2000. Acceleration of global warming due to carbon-cycle feedbacks in a coupled climate model. Nature 408, 184–187.

Cramer, W., Bondeau, A., Woodward, F.I., Prentice, I.C., Betts, R.A., Brovkin, V., Cox, P.M., Fisher, V., Foley, J.A., Friend, A.D., Kucharik, C., Lomas, M.R., Ramankutty, N., Sitch, S., Smith, B., White, A., Young-Molling, C., 2001. Global response of terrestrial ecosystem structure and function to CO_2 and climate change: results from six dynamic global vegetation models. Glob. Change Biol. 7, 357–373.

Daly, C., Bachelet, D., Lenihan, J.M., Neilson, R.P., Parton, W.J., Ojima, D., 2000. Dynamic simulation of tree-grass interactions for global change studies. Ecol. Appl. 10, 449–469.

Doherty, R., Kutzbach, J., Foley, J., Pollard, D., 2000. Fully coupled climate/dynamical vegetation model simulations over northern Africa during the mid-Holocene. Clim. Dyn. 16, 561–573.

Efron, B., Tibshirani, R.J., 1993. An Introduction to the Bootstrap. Chapman & Hall, New York, 436 pp.

Emanuel, W.R., Shugart, H.H., Stevenson, M.P., 1985. Climatic change and the broad-scale distribution of terrestrial ecosystem complexes. Clim. Change 7, 29–43.

Foley, J.A., Levis, S., Prentice, I.C., Pollard, D., Thompson, S.L., 1998. Coupling dynamic models of climate and vegetation. Glob. Change Biol. 4, 561–579.

Foley, J.A., Prentice, I.C., Ramankutty, N., Levis, S., Pollard, D., Sitch, S., Haxeltine, A., 1996. An integrated biosphere of land surface processes, terrestrial carbon balance, and vegetation dynamics. Glob. Biogeochem. Cycles 10, 603–628.

Friend, A.D., Stevens, A.K., Knox, R.G., Cannell, M.G.R., 1997. A process-based, terrestrial biosphere model of ecosystems dynamics (Hybrid v3.0). Ecol. Model. 95, 249–287.

Fu, C.B., Wen, G., 1999. Variation of ecosystems over East Asia in association with seasonal, interannual and decadal monsoon climate variability. Clim. Change 43, 477–494.

Gagan, M.K., Ayliffe, L.K., Hopley, D., Cali, J.A., Mortimer, G.E., Chappell, J., McCulloch, M.T., Head, M.J., 1998. Temperature and surface-ocean water balance of the mid-Holocene tropical Western Pacific. Science 279, 1014–1018.

Gallimore, R., Prentice, I.C., Jacob, R., Kutzbach, J.E., 2005. Simulations of pre-industrial and mid-Holocene climates using a fully coupled climate model with dynamic vegetation. Clim. Dyn., in preparation.

Ganopolski, A., Kubatzki, C., Claussen, M., Brovkin, V., Petoukhov, V., 1998. The influence of vegetation–atmosphere–ocean interaction on climate during the mid-Holocene. Science 280, 1916–1919.

Gasse, F., Van Campo, E., 1994. Abrupt post-glacial climate events in West Asia and North Africa monsoon domains. Earth Planet. Sci. Lett. 126, 435–456.

Gauslaa, Y., 1984. Heat resistance and energy budget in different Scandinavian plants. Holarctic Ecol. 7, 3–78.

Goldammer, J.G., Seibert, B., 1990. The impact of droughts and forest fires on tropical lowland rain forest of east Kalimantan. In: Goldammer, J.G. (Ed.), Fire in the Tropical Biota: Ecosystem Processes and Global Challenges. Springer-Verlag, New York, pp. 11–31.

Grau, H.R., Veblen, T.T., 2000. Rainfall variability, fire and vegetation dynamics in neotropical montane ecosystems in northwestern Argentina. J. Biogeogr. 27, 1107–1121.

Gurvich, D.E., Cabido, M., Thorpe, P.C., Diaz, S., Falczuk, V., Pérez-Harguindeguy, N., 2002. Foliar resistance to simulated extreme temperature events in contrasting plant functional and chorological types. Glob. Change Biol. 8, 1139–1145.

Harrison, S.P., Kutzbach, J.E., Liu, Z., Bartlein, P.J., Otto-Bliesner, B., Muhs, D., Prentice, I.C., Thompson, R.S., 2003. Mid-Holocene climate of the Americas: a dynamical response to changed seasonality. Clim. Dyn. 20, 663–688.

Harrison, S.P., Prentice, I.C., 2003. Climate and CO_2 controls on global vegetation distribution at the last glacial maximum: analysis based on palaeovegetation data, biome modeling and palaeoclimate simulations. Glob. Change Biol. 9, 983–1004.

Haxeltine, A., Prentice, I.C., 1996. BIOME3: an equilibrium terrestrial biosphere model based on ecophysiological constraints, resource availability, and competition among plant functional types. Glob. Biogeochem. Cycles 10, 693–709.

Heimann, M., Esser, G., Haxeltine, A., Kaduk, J., Kicklighter, D.W., Knorr, W., Kohlmaier, G.H., McGuire, A.D., Melillo, J., Moore III, B., Otto, R.D., Prentice, I.C., Sauf, W., Schloss, A., Sitch, S., Wittenberg, U., Würth, G., 1998. Evaluation of terrestrial carbon cycle models through simulations of the seasonal cycle of atmospheric CO_2: first results of a model intercomparison study. Glob. Biogeochem. Cycles 12, 1–24.

Hessl, A.E., McKenzie, D., Schellhaas, R., 2004. Drought and Pacific decadal oscillation linked to fire occurrence in the inland Pacific Northwest. Ecol. Appl. 14, 425–442.

Hewitt, C., Mitchell, J., 1998. A fully coupled GCM simulation of the climate of the mid-Holocene. Geophys. Res. Lett. 25, 361–364.

Higgins, R.W., Shi, W., 2001. Intercomparison of the principal modes of interannual and intraseasonal variability of the North American monsoon system. J. Clim. 14, 403–417.

Holdridge, L.R., 1967. Life Zone Ecology. Tropical Science Center, San Jose, Costa Rica, 206 pp.

Hulme, M., 2001. Climatic perspectives on Sahelian desiccation: 1973–1998. Glob. Environ. Change 11, 19–29.

Hulme, M., Doherty, R., Ngara, T., New, M., Lister, D., 2001. African climate change: 1900–2100. Clim. Res. 17, 145–168.

Huntingford, C., Cox, P.M., Lenton, T.M., 2000. Contrasting responses of a simple terrestrial ecosystem model to global change. Ecol. Model. 134, 41–58.

Hutchinson, M.F., 1995. Interpolating mean rainfall using thin-plane smoothing splines. Int. J. Geogr. Inform. Syst. 9, 385–403.

Hutchinson, M.F., Bischof, R.J., 1983. A new method for estimating the spatial distribution of mean seasonal and annual rainfall applied to the Hunter Valley, New South Wales. Aust. Meteorol. Mag. 31, 179–184.

Jacob, R., Schafer, C., Foster, I., Robis, M., Anderson, J., 2001. Computational design and performance of the Fast Ocean Atmosphere Model, version one. In: Alexandrov, V.N., Dongarra, J.J., Tan, C.J.K. (Eds.), Proceeding of the 2001 International Conference on Computational Science. Springer-Verlag, Berlin, pp. 175–184.

Jacob, R.L., 1997. Low frequency variability in a simulated atmosphere ocean system. Ph.D. Thesis. University of Wisconsin-Madison, Madison, 159 pp.

Jolly, D., Harrison, S.P., Damnati, B., Bonnefille, R., 1998a. Simulated climate and biomes of Africa during the late quaternary: comparison with pollen and lake status data. Quaternary Sci. Rev. 17, 629–657.

Jolly, D., Prentice, C.I., Bonnefille, R., Ballouche, A., Bengo, M., Brenac, P., Buchet, G., Burney, D., Cazet, J.-P., Cheddadi, R., Edorh, T., Elenga, H., Elmoutaki, S., Guiot, J., Laarif, F., Lamb, H., Lezine, A.-M., Maley, J., Mbenza, M., Peryon, O., Reille, M., Reynaud-Farrera, I., Riollet, G., Ritchie, J.C., Roche, E., Scott, L., Ssemmanda, I., Straka, H., Umer, M., Van Campo, E., Vilimumbalo, S., Vincens, A., Waller, M., 1998b. Biome reconstruction from pollen and plant macrofossil data for Africa and the Arabian Peninsula at 0 and 6000 years. J. Biogeogr. 25, 1007–1027.

Joussaume, S., Braconnot, P., 1997. Sensitivity of paleoclimate simulation results to season definitions. J. Geophys. Res. Atmos. 102, 1943–1956.

Joussaume, S., Taylor, K.E., Braconnot, P., Mitchell, J.F.B., Kutzbach, J.E., Harrison, S.P., Prentice, I.C., Broccoli, A.J., Abe-Ouchi, A., Bartlein, P.J., Bonfils, C., Dong, B., Guiot, J., Herterich, K., Hewitt, C.D., Jolly, D., Kim, J.W., Kislov, A., Kitoh, A., Loutre, M.F., Masson, V., McAvaney, B., McFarlane, N., de Noblet, N., Peltier, W.R., Peterschmitt, J.Y., Pollard, D.,

Rind, D., Royer, J.F., Schlesinger, M.E., Syktus, J., Thompson, S., Valdes, P., Vettoretti, G., Webb, R.S., Wyputta, U., 1999. Monsoon changes for 6000 years ago: results of 18 simulations from the Paleoclimate Modeling Intercomparison Project (PMIP). Geophys. Res. Lett. 26, 859–862.

Justice, C.O., Kendall, J.D., Dowty, P.R., Scholes, R.J., 1996. Satellite remote sensing of fires during the SAFARI campaign using NOAA advanced very high resolution radiometer data. J. Geophys. Res. 101, 23851–23864.

Karl, T.R., Knight, R.W., Plummer, N., 1995. Trends in high-frequency climate variability in the twentieth century. Nature 377, 217–220.

Kicklighter, D.W., Bruno, M., Donges, S., Esser, G., Heimann, M., Helfrich, J., Ift, F., Joos, F., Kaduk, J., Kohlmaier, G.H., McGuire, A.D., Melillo, J.M., Meyer, R., Moore, B., Nadler, A., Prentice, I.C., Sauf, W., Schloss, A.L., Sitch, S., Wittenberg, U., Wurth, G., 1999. A first-order analysis of the potential role of CO_2 fertilization to affect the global carbon budget: a comparison of four terrestrial biosphere models. Tellus B 51, 343–366.

Kohfeld, K.E., Harrison, S.P., 2000. How well can we simulate past climates? Evaluating the models using global palaeoenvironmental datasets. Quaternary Sci. Rev. 19, 321–346.

Kucharik, C.J., Foley, J.A., Delire, C., et al., 2000. Testing the performance of a dynamic global ecosystem model: water balance, carbon balance, and vegetation structure. Glob. Biogeochem. Cycles 14, 795–825.

Kutzbach, J.E., Gallimore, R., Harrison, S.P., Behling, P., Selin, R., Laarif, F., 1998. Climate and biome simulations for the past 21,000 years. Quaternary Sci. Rev. 17, 473–506.

Kutzbach, J.E., Gallimore, R.G., 1988. Sensitivity of a coupled atmosphere mixed layer ocean model to changes in orbital forcing at 9000 years BP. J. Geophys. Res. Atmos. 93, 803–821.

Kutzbach, J.E., Harrison, S.P., Coe, M.T., 2001. Land–ocean–atmosphere interactions and monsoon climate change: a palaeoperspective. In: Schulze, E.-D., Heimann, M., Harrison, S.P., Holland, E., Lloyd, J., Prentice, I.C., Schimel, D.S. (Eds.), Global Biogeochemical Cycles in the Climate System. Academic Press, San Diego, pp. 73–86.

Larcher, W., 2003. Physiological Plant Ecology. Springer-Verlag, Berlin.

Liu, Z., Harrison, S.P., Kutzbach, J., Otto-Bliesner, B., 2004. Global monsoons in the mid-Holocene and oceanic feedback. Clim. Dyn. 22, 157–182.

Liu, Z., Jacob, R., Kutzbach, J.E., Harrison, S.P., Anderson, J., 1999. Monsoon impact on El Niño in the Early Holocene. PAGES Newslett. 7, 16–17.

Liu, Z., Kutzbach, J.E., Wu, L., 2000. Modeling climatic shift of El Niño variability in the Holocene. Geophys. Res. Lett. 27, 2265–2268.

Liu, Z., Wu, L., 2000. Tropical Atlantic variability in a coupled GCM. Atmos. Sci. Lett. 1, 26–36.

Liu, Z., Wu, L., Gallimore, R., Jacob, R., 2002. Search for the origins of Pacific decadal climate variability. Geophys. Res. Lett. 29, doi:10.1029/2001GL013735.

Los, S.O., Collatz, G.J., Bounoua, L., Sellers, P.J., Tucker, C.J., 2001. Global interannual variations in sea surface temperature and land surface vegetation, air temperature, and precipitation. J. Clim. 14, 1535–1549.

Lucht, W., Prentice, I.C., Myneni, R.B., Sitch, S., Friedlingstein, P., Cramer, W., Bousquet, P., Buermann, W., Smith, B., 2002. Climatic control of the high-latitude vegetation greening trend and Pinatubo effect. Science 296, 1687–1689.

McGlone, M.S., Kershaw, A.P., Markgraf, V., 1992. El Niño/southern oscillation climatic variability in Australasia and South America palaeoenvironmental records. In: Diaz, H.F., Markgraf, V. (Eds.), El Niño: Historical and Paleoclimatic Aspects of the Southern Oscillation. Cambridge University Press, Cambridge, pp. 435–462.

McGuire, A.D., Sitch, S., Clein, J.S., Dargaville, R., Esser, G., Foley, J., Heimann, M., Joos, F., Kaplan, J., Kicklighter, D.W., Meier, R.A., Melillo, J.M., Moore, B., Prentice, I.C., Ramankutty, N., Reichenau, T., Schloss, A., Tian, H., Williams, L.J., Wittenberg, U., 2001. Carbon balance of the terrestrial biosphere in the twentieth century: analyses of CO_2, climate and land use effects with four process-based ecosystem models. Glob. Biogeochem. Cycles 15, 183–206.

Mitchell, J.F.B., Grahame, N.S., Needham, K.J., 1988. Climate simulations for 9000 years before present: seasonal variations and effect of the Laurentide ice sheet. J. Geophys. Res. Atmos. 93, 8283–8303.

Monahan, A.H., Fyfe, J.C., Flato, G.M., 2000. A regime view of northern hemisphere atmospheric variability and change under global warming. Geophys. Res. Lett. 27, 1139–1142.

Neilson, R.P., 1995. A model for predicting continental scale vegetation distribution and water balance. Ecol. Appl. 5, 362–385.

New, M., Hulme, M., Jones, P.D., 1999. Representing twentieth-century space-time climate variability. Part I. Development of a 1961–90 mean monthly terrestrial climatology. J. Clim. 12, 829–856.

New, M., Hulme, M., Jones, P.D., 2000. Representing twentieth-century space-time climate variability. Part II. Development of 1961–96 monthly grids of terrestrial surface climate. J. Clim. 13, 2217–2238.

Ni, J., Sykes, M.T., Prentice, I.C., Cramer, W., 2000. Modelling the vegetation of China using the process-based equilibrium terrestrial biosphere model BIOME3. Glob. Ecol. Biogeogr. 9, 463–479.

Ni, J., Yu, G., Harrison, S.P., Prentice, I.C., 2005. Pollen-based reconstruction of vegetation in China during the mid-Holocene and last glacial maximum using a global scheme of plant functional types. J. Veg. Sci. submitted for publication.

Nicholson, S.E., 2000. The nature of rainfall variability over Africa on time scales of decades to millennia. Glob. Planet. Change 26, 137–158.

Oba, G., Post, E., Stenseth, N.C., 2001. Sub-Saharan desertification and productivity are linked to hemispheric climate variability. Glob. Change Biol. 7, 241–246.

Olson, J.R., Baum, B.A., Cahoom, D.R., Crawford, J.H., 1999. Frequency and distribution of forest, savanna, and crop fires over tropical regions during PEM-Tropical A. J. Geophys. Res. 104, 5865–5876.

Otto-Bliesner, B.L., 1999. El Niño/La Niña and Sahel precipitation during the mid-Holocene. Geophys. Res. Lett. 26, 87–90.

Plisnier, P.D., Serneels, S., Lambin, E.F., 2000. Impact of ENSO on East African ecosystems: a multivariate analysis based on climate and remote sensing data. Glob. Ecol. Biogeogr. 9, 481–497.

Prentice, I.C., 2001. Interactions of climate change and the terrestrial biosphere. In: Bengtsson, L.O., Hammer, C.U. (Eds.), Geosphere–Biosphere Interactions and Climate. Pontifical Academy of Sciences. Cambridge University Press, Cambridge, pp. 176–195.

Prentice, I.C., Cramer, W., Harrison, S.P., Leemans, R., Monserud, R.A., Solomon, A.M, 1992. A global biome model based on plant physiology and dominance, soil properties and climate. J. Biogeogr. 19, 117–134.

Prentice, I.C., Heimann, M., Sitch, S., 2000a. The carbon balance of the terrestrial biosphere: ecosystem models and atmospheric observations. Ecol. Appl. 10, 1553–1573.

Prentice, I.C., Jolly, D., BIOME 6000 Participants, 2000b. Mid-Holocene and glacial-maximum vegetation geography of the northern continents and Africa. J. Biogeogr. 27, 507–519.

Raunkiaer, C., 1934. The Life-forms of Plants and Statistical Plant Geography. Clarendon Press, Oxford, 632 pp.

Roberts, N., Wright Jr., H.E., 1993. Vegetational, lake-level, and climatic history of the Near East and Southwest Asia. In: Wright Jr., H.E., Kutzbach, J.E., Webb III, T., Ruddiman, W.F., Street-Perrott, F.A., Bartlein, P.J. (Eds.), Global Climates since the Last Glacial Maximum. University of Minnesota Press, Minneapolis, pp. 194–220.

Rodbell, D.T., Seltzer, G.O., Anderson, D.M., Abbott, M.B., Enfield, D.B., Newman, J.H., 1999. An ∼15,000-year record of El Niño-driven alluviation in southwestern Ecuador. Science 283, 516–520.

Sandweiss, D.H., Richardson III, J.B., Reitz, E.J., Rollins, H.B., Maasch, K.A., 1996. Geoarchaeological evidence from Peru for a 5000 years BP onset of El Niño. Science 273, 1531–1533.

Shulmeister, J., Lees, B.G., 1995. Pollen evidence from tropical Australia for the onset of an ENSO-dominated climate at c. 4000 BP. The Holocene 5, 10–18.

Sitch, S., Smith, B., Prentice, I.C., Arneth, A., Bondeau, A., Cramer, W., Kaplan, J.O., Levis, S., Lucht, W., Sykes, M.T., Thonicke, K., Venevsky, S., 2003. Evaluation of ecosystem dynamics, plant geography and terrestrial carbon cycling in the LPJ dynamic global vegetation model. Glob. Change Biol. 9, 161–185.

Street, F.A., Grove, A.T., 1976. Environmental and climatic implications of Late Quaternary lake-level fluctuations in Africa. Nature 261, 385–390.

Street-Perrott, F.A., Harrison, S.P., 1985. Lake levels and climate reconstruction. In: Hecht, A.D. (Ed.), Paleoclimate Analysis and Modeling. Wiley, New York, pp. 291–340.

Street-Perrott, F.A., Marchand, D.S., Roberts, N., Harrison, S.P., 1989. Global Lake-level variations from 18,000 to 0 years ago: a palaeoclimatic analysis. U.S. Department of Energy DOE/ER/60304-H1, Technical Report TR046, 213 pp.

Street-Perrott, F.A., Perrott, R.A., 1993. Holocene vegetation, lake levels, and climate of Africa. In: Wright Jr., H.E., Kutzbach, J.E., Webb III, T., Ruddiman, W.F., Street-Perrott, F.A., Bartlein, P.J. (Eds.), Global Climates since the Last Glacial Maximum. University of Minnesota Press, Minneapolis, pp. 318–356.

Thompson, L.G., Davids, M.E., Mosley-Thompson, E., Sowers, T.A., Henderson, K.A., Zagorodnov, V.S., Lin, P.N., Mikhalenko, V.N., Campen, R.K., Bolzan, J.F., Cole-Dai, J.A., Francou, B., 1998. A 25,000-year tropical climate history from Bolivian ice cores. Science 282, 1858–1864.

Thompson, L.G., Mosley-Thompson, E., Henderson, K.A., 2000. Ice-core palaeoclimate records in tropical South America since the Last Glacial Maximum. J. Quaternary Sci. 15, 377–394.

Thonicke, K., Venevsky, S., Sitch, S., Cramer, W., 2001. The role of fire disturbance for global vegetation dynamics: coupling fire into a Dynamic Global Vegetation Model. Glob. Ecol. Biogeogr. 10, 661–667.

Tudhope, A.W., Chilcott, C.P., McCulloch, M.T., Cook, E.R., Chappell, J., Ellam, R.M., Lea, D.W., Lough, J.M., Shimmield, G.B., 2001. Variability in the El Niño-Southern Oscillation through a Glacial-Interglacial cycle. Science 291, 1511–1517.

Wang, G.L., Eltahir, E.A.B., 2000. Role of vegetation dynamics in enhancing the low-frequency variability of the Sahel rainfall. Water Resour. Res. 36, 1013–1021.

Winkler, M.G., Wang, P.K., 1993. The late-Quaternary vegetation and climate of China. In: Wright Jr., H.E., Kutzbach, J.E., Webb III, T., Ruddiman, W.F., Street-Perrott, F.A., Bartlein, P.J. (Eds.), Global Climates since the Last Glacial Maximum. University of Minnesota Press, Minneapolis, pp. 221–264.

Wohlfahrt, J., Harrison, S.P., Braconnot, P., 2004. Synergistic feedbacks between ocean and vegetation on mid- and high-latitude climates during the mid-Holocene. Clim. Dyn. 22, 223–238.

Wohlfahrt, J., Harrison, S.P., Braconnot, P., Hewitt, C.D., Kitoh, A., Mikolajewicz, U., Otto-Bliesner, B., Weber, N., 2005. Evaluation of coupled ocean–atmosphere simulations of northern hemisphere extratropical climates in the mid-Holocene. Clim. Dyn., submitted for publication.

Woodward, F.I., 1987. Climate and Plant Distribution. Cambridge University Press, Cambridge, 174 pp.

Woodward, F.I., 1988. Temperature and the distribution of plant species. In: Long, S.P., Woodward, F.I. (Eds.), Plants and Temperature. Symposia of the Society for Experimental Biology, vol. 42. Company of Biologists, Cambridge, pp. 59–75.

Woodward, F.I., Kelly, C.K., 1997. Plant functional types: towards a definition by environmental constraints. In: Smith, T.M., Shugart, H.H., Woodward, F.I. (Eds.), Plant Functional Types. Cambridge University Press, Cambridge, pp. 47–65.

Woodward, F.I., Lomas, M.R., Betts, R.A., 1998. Vegetation-climate feedbacks in a greenhouse world. Philos. Trans. Roy. Soc. London Ser. B 353, 29–38.

Wu, L., Liu, Z., 2003. Decadal variability in the North Pacific: the eastern North Pacific mode. J. Clim. 16, 3111–3131.

Wu, L., Liu, Z., Gallimore, R., Jacob, R., Lee, D., Zhong, Y., 2003. Pacific decadal variability: the tropical Pacific mode and the North Pacific mode. J. Clim. 16, 1101–1120.

Yu, G., Chen, X., Ni, J., Cheddadi, R., Guiot, J., Han, H., Harrison, S.P., Huang, C., Ke, M., Kong, Z., Li, S., Li, W., Liew, P., Liu, G., Liu, J., Liu, K.-B., Prentice, I.C., Qui, W., Ren, G., Song, C., Sugita, S., Sun, X., Tang, L., van Campo, E., Xia, Y., Xu, Q.,

Yan, S., Yang, X., Zhao, J., Zheng, Z., 2000. Palaeovegetation of China: a pollen data-based synthesis for the mid-Holocene and last glacial maximum. J. Biogeogr. 27, 635–664.

Yu, G., Prentice, I.C., Harrison, S.P., Sun, X., 1998. Pollen-bases biome reconstructions for China at 0 and 6000 years. J. Biogeogr. 25, 1055–1069.

Zeng, N., Neelin, J.D., 2000. The role of vegetation–climate interaction and interannual variability in shaping the African savanna. J. Clim. 13, 2665–2670.

Zeng, N., Neelin, J.D., Lau, K.M., Tucker, C.J., 1999. Enhancement of interdecadal climate variability in the Sahel by vegetation interaction. Science 286, 1537–1540.